Journal of Mining Science, Vol. 40, No. 6, 2004

MODELING OF WAVE PROPAGATION IN BLOCK MEDIA

N. I. Aleksandrova and E. N. Sher UDC 550.834 + 622.831

Propagation of strain waves is experimentally investigated under impact loading of a rod system composed of steel cylinders separated by pliable interlayers. The existence of pendulum-type waves is confirmed. In order that wave process in the rod system is numerically described, a viscoelastic model of deforming materials of interlayers used in the experiment is constructed. It is shown that the velocity of waves and the degree of their attenuation are to a great extent dependent on viscous properties of the material of interlyers.

Impact, wave, deformation, block medium, interlayer, elasticity, viscosity

Rocks are characterized by block structure, which is run down on various scale levels from crystal grains to rock mass block separated by large faults [1]. On some levels, blocks get detached by joints with weakened mechanical properties, which affects the process of wave propagation in such medium [2]. It has been shown that in block medium, wave groups named pendulum waves propagate with velocities that are far less than velocities of longitudinal waves [3 – 5]. This is explained by oscillation developing in a chain of stiff blocks interacting by pliable interlayers. Process of wave propagation in one-dimensional physical model constructed with the use of silicate bricks and organic glass blocks is investigated in [4].

In the present paper, block structure was modeled by steel rods 25 mm in diameter and 100 mm in length separated by interlayers made of dense and porous sheet resin, linoleum, and foam plastic. The steel rod are advantageous for possible use of one-dimensional deformation schemes when modeling theoretically wave propagation in the *rods — interlayers* chain.

EXPERIMENTAL MODELING OF WAVE PROPAGATION IN A COMPOUND ROD SYSTEM

The rods separated by interlayers were arranged in a vertical pipe with longitudinal openings to outlet cables of sensors recording characteristics of movement. Accelerometers lengthwise embedded into some rods served as the sensors. The rods were distributed along the upper part of the assemblage. Impact was delivered on the free end of the upper rod, the impact parameters were recorded by accelerometer mounted on striker. Due to the assemblage length of 2 m, it was possible to record oscillations prior to arrival of waves reflected from the lower part of the assemblage.

Material of interlayers, duration of loading impact pulse, and the pulse amplitude were varied. Some experiments were conducted under conditions when the assemblage of interlayered rods was tightened by external rubber tractions.

The data obtained in the experiments were characterized by two distinguished types of waves: low-frequency waves and lagging high-frequency waves. The latter have a frequency of 25 kHz that coincides with the natural frequency of a steel rod 100 mm in length.

Institute of Mining, Siberian Branch, Russian Academy of Sciences, Novosibirsk, Russia. Translated from Fiziko-Tekhnicheskie Problemy Razrabotki Poleznykh Iskopaemykh, No. 6, pp. 49-57, November-December, 2004. Original article submitted November 10, 2004.

1062-7391/04/4006-0579

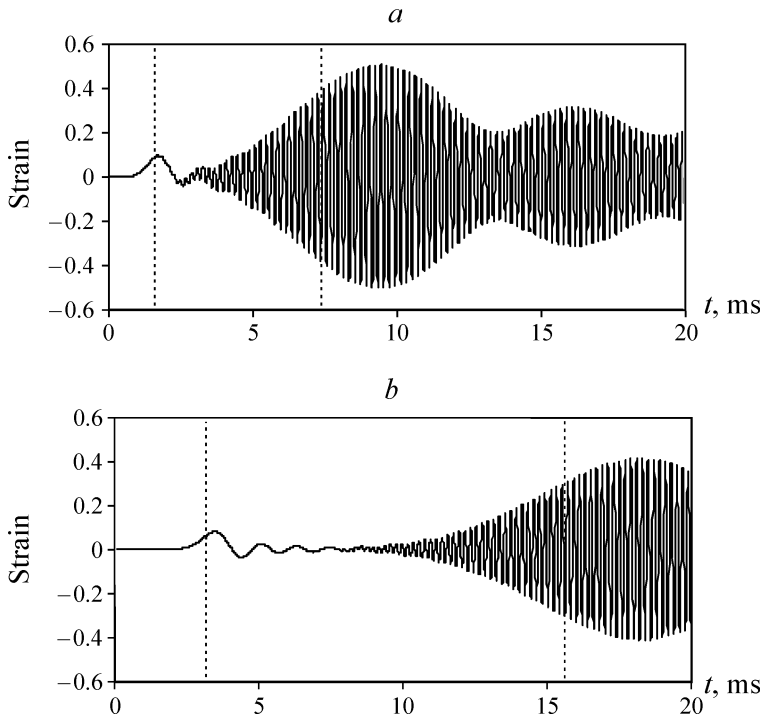

Fig. 1. Strain in (*a*) the fifth and (*b*) the tenth rod in the system after impact

Such behavior of waves in a compound *elastic rods — springs* system was qualitatively determined in [6], where propagation of impact-generated waves was investigated analytically and numerically for linearly elastic springs. Figure 1 demonstrates an example of calculating strains in rods after short-duration impact.

As distinct from theoretical results, in the experiments, more intensive attenuation of waves is observed. This is especially particular for the high-frequency waves that attenuate very strongly and are recorded practically on the first three rods. Under short impact pulse, the amplitudes of the waves are larger and the waves propagate father as rigidity of interlayers increases. In Fig. 2*a*, *b*, *c* the oscillograms are presented for accelerations of the first, third, and eleventh rods in a compound system with dense rubber interlayers.

Another difference between the experimental and theoretical data was a considerable discordance in the velocities of low-frequency waves. The theoretical results obtained with the static rigidities of interlayers appeared to be several times less than the experimental ones. This may be explained by inelastic behavior of interlayers, and their deformation properties were therefore investigated at various loading rates. Loading was carried out at the strain rate $\dot{\varepsilon} = 5 \cdot 10^{-3} - 1 \text{ s}^{-1}$. The test showed that linoleum and dense rubber (Fig. 3) are characterized by a nonlinear growth of Young's modulus, hysteresis under unload, and a pronounced effect of the strain rate on the loading diagram shape. In case of porous rubber and foam plastic, the loading rate influence was minor, as well as the branches of loading and unload differed weakly.

The experimental data for the rigidity of interlayer at the compression force of 120 N are presented in Table 1. The static rigidity K_{st} corresponds to the minimal loading rate $\dot{\varepsilon} = 5 \cdot 10^{-3} \text{ s}^{-1}$, the dynamic rigidity K_d is determined at $\dot{\varepsilon} = 1.2 \text{ s}^{-1}$.

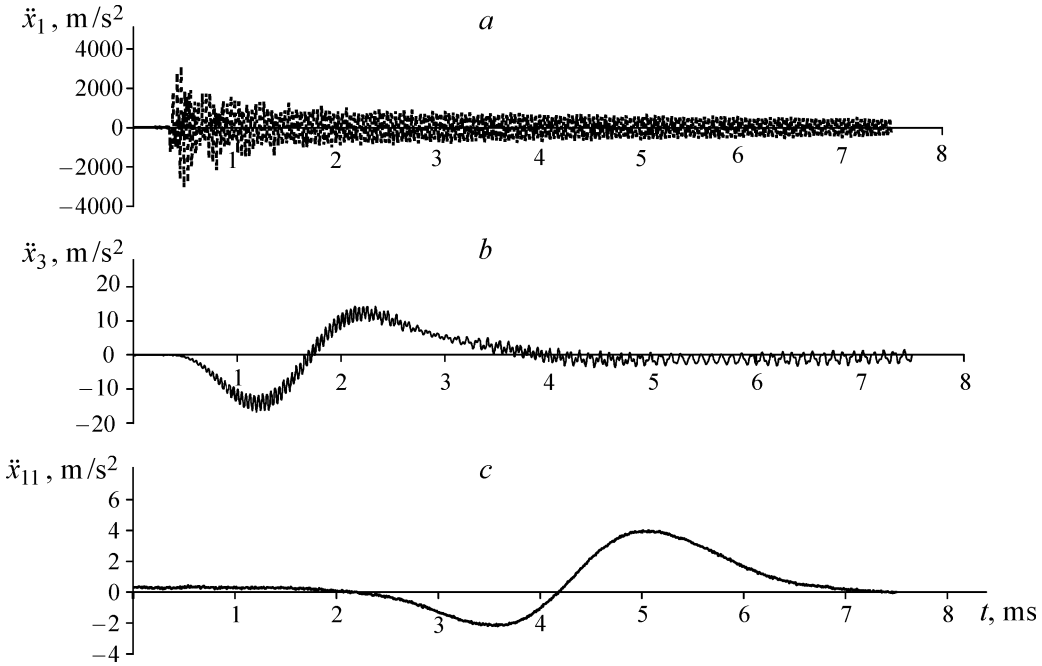

Fig. 2. Experimental oscillograms of accelerations of the first, third, and eleventh rods at short impact pulse

A faster loading at $\dot{\varepsilon} = 10 - 50\ \ \mathrm{s}^{-1}$ was conducted at an impact stand shown schematically in Fig. 4. Test-subjected interlayer *1* was placed between two rods *2* and *3*; lower rod *3* was able to displace freely in holder *4*. Upper rod *2* was equipped with accelerometer *5*. When the system was lifted and dropped, the lower rod hit on the massive basement, and then the upper rod oscillation began and was recorded by the accelerometer.

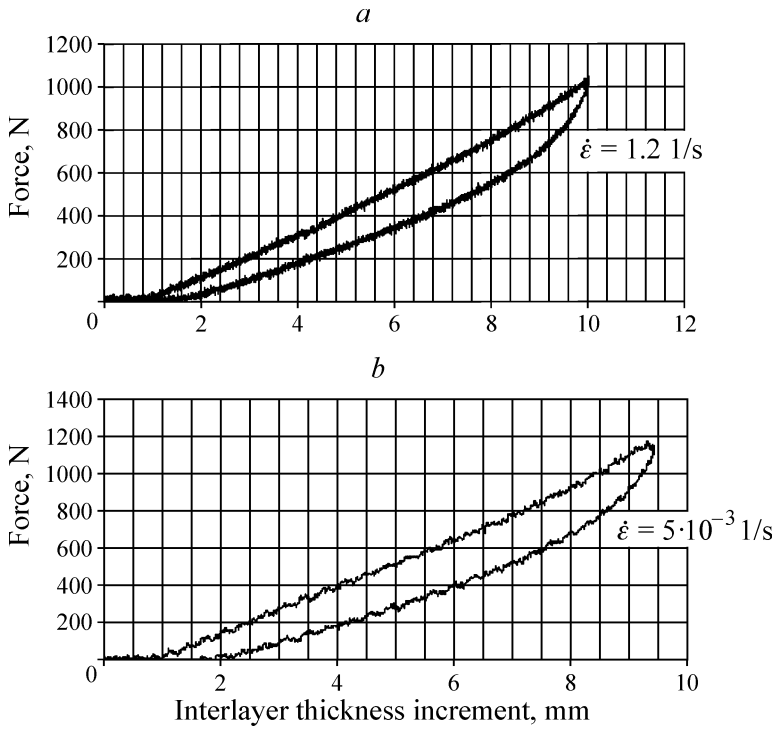

Fig. 3. Compression diagrams for dense rubber interlayer at different loading rates

TABLE 1

Material	K_{st}, kN/m	K_d, kN/m	K_s, kN/m	K_V, kN/m	C_{st}, m/s	C_V, m/s	λ_1, kg/s	λ_2, kg/s
Dense rubber	480	620	1200	4400	110	340	10000	500
Porous rubber	16	16	16	170	20	75	1000	10
Linoleum	80	180	500	4600	45	340	10000	500
Foam plastic	350	350		500	93	115	1000	10

To analyze the data of such tests, the impact stand operation was modeled with replacing the rods by the masses m_1 and m_2, and the interlayer, by a spring with a desired rigidity K_s (Fig. 5). Rod *3* had a spherically rounded lower end, which allowed Hertz's interaction law, being governed by the coefficient C, to be used in the calculation scheme [7]. The upper rod acceleration $\ddot{x}_1(t)$ was found from a solution of the system of differential equations:

$$m_1\ddot{x}_1 = m_1 g - (x_1 - x_2)K_s,$$
$$m_2\ddot{x}_2 = m_2 g - C\,x_2^{1.5} + (x_1 - x_2)K_s \qquad (1)$$

with the following initial conditions at $t = 0$: $x_1 = x_2 = 0$, $\dot{x}_1 = \dot{x}_2 = V_0$, where x_2 is the displacement of the second rod, and V_0 is the velocity of rods at the pre-impact moment. By oscillograms of $\ddot{x}_1(t)$, a period of time from the pulse onset to the signal minimum T_p was determined. With the help of T_p and solution of (1), the interlayer rigidities K_s were calculated, the values of which are cited in Table 1. It is evident that the rigidity of dense rubber and linoleum increases markedly when the strain rate rises. This effect is less observed in porous rubber and foam plastic. The nonlinear properties of interlayer deformation were described using a model combining elastic and viscous elements as is demonstrated in Fig. 6.

The compression forces F of the elastic and viscous elements are determined by the relations $F = K\delta$ and $F = \lambda\dot{\delta}$, respectively; here, δ is the element extension, K is the rigidity, and λ is the viscosity coefficient. If the elastic and viscous elements are connected consecutively, then F is calculated from the equation $\dot{F}/K_1 + F/\lambda_1 = \dot{\delta}$. After its integration, obtain:

$$F(t) = K_1 \int_0^t e^{-\alpha_1 t}\dot{\delta}\,dt, \quad \alpha_1 = \frac{K_1}{\lambda_1}.$$

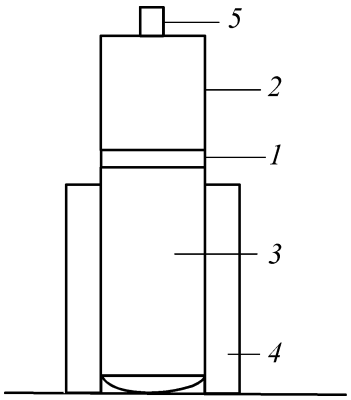

Fig. 4

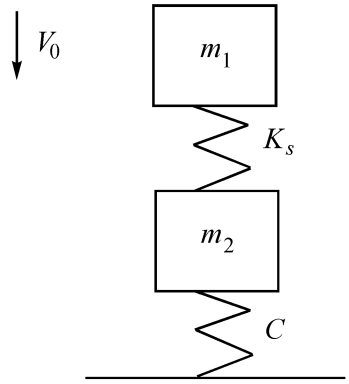

Fig. 5

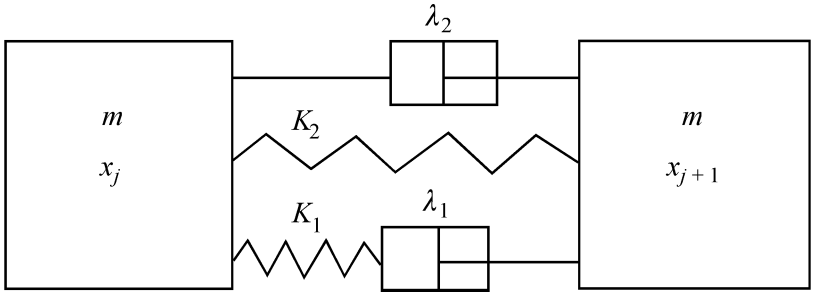

Fig. 6. Viscoelastic model of interlayer

When the elements in question are connected in parallel to one another, the forces acting from each element side are summed. As a result, for model in Fig. 6, the force F_j^r that affects the mass with a coordinate x_j from the right is expressed by the formula:

$$F_j^r = K_2(x_{j+1} - x_j) + \lambda_2(\dot{x}_{j+1} - \dot{x}_j) + K_1 e^{-\alpha_1 t} \int_0^t e^{\alpha_1 t}(\dot{x}_{j+1} - \dot{x}_j)\, dt\,. \tag{2}$$

An analogous equation exists for the force F_j^l that acts from the left. Using the motion law $m\ddot{x}_j = F_j^r - F_j^l$, a system of equations describing the movement of masses in a compound assemblage is derived:

$$m\ddot{x}_j = K_2(x_{j-1} - 2x_j + x_{j+1}) + \lambda_2(\dot{x}_{j-1} - 2\dot{x}_j + \dot{x}_{j+1}) + K_1 e^{-\alpha_1 t} \int_0^t e^{\alpha_1 t}(\dot{x}_{j-1} - 2\dot{x}_j + \dot{x}_{j+1})\, dt\,. \tag{3}$$

When loadings are slow, the forces of the viscous element are small, and the behavior of interlayer is dependent on the elastic element with K_2. Thus, it can be assumed that $K_2 = K_{st}$. When loading rates are great, interlayer rigidity approaches $K_V = K_1 + K_2$. The parameters K_1, λ_1, and λ_2 of the interlayer model from Fig. 6 are unknown. In the present paper, their values were selected basing on a condition of the best agreement between the experimental and theoretical data. Peculiar attention was given to correspondence of values of low-frequency wave propagation velocity, its period, and attenuation coefficient.

THEORETICAL MODEL OF WAVE PROPAGATION IN A CHAIN OF RODS

Consider a model of a system of identical elastic rods with interlayers between one another. The rods have the following parameters: ρ is the density, E is Young's modulus, $c = \sqrt{E/\rho}$ is the longitudinal velocity, y is the length, and S is the cross-section. The equations of the rod movement has the form :

$$\ddot{u}_j = c^2 u_j''; \quad j = 0,..., J\,, \tag{4}$$

where u_j is the jth rod displacement, the prime denotes a derivative with respect to the coordinate x. The interlayers are modeled similarly to the case of the chains of masses (Fig. 6). All interlayers between the rods are identical. According to (2) the forces F_j^r and F_j^l, that affect the jth rod from the right and from the left, respectively, are calculated from the formulae:

$$SEu'_j\big|_{x=y(j-1/2)} = F_j^l = -K_2(u_{j-1}\big|_{x=y(j-1/2)} - u_j\big|_{x=y(j-1/2)}) - \lambda_2(\dot{u}_{j-1}\big|_{x=y(j-1/2)} - \dot{u}_j\big|_{x=y(j-1/2)})$$
$$- K_1 e^{-\alpha_1 t}\int_0^t e^{\alpha_1 t}(\dot{u}_{j-1}\big|_{x=y(j-1/2)} - \dot{u}_j\big|_{x=y(j-1/2)})\,dt; \quad j = 1,..., J;$$
$$SEu'_j\big|_{x=y(j+1/2)} = F_j^r = K_2(u_{j+1}\big|_{x=y(j+1/2)} - u_j\big|_{x=y(j+1/2)}) + \lambda_2(\dot{u}_{j+1}\big|_{x=y(j+1/2)} - \dot{u}_j\big|_{x=y(j+1/2)}) \tag{5}$$
$$+ K_1 e^{-\alpha_1 t}\int_0^t e^{\alpha_1 t}(\dot{u}_{j+1}\big|_{x=y(j+1/2)} - \dot{u}_j\big|_{x=y(j+1/2)})\,dt; \quad j = 0,..., J-1.$$

Let the $(J+1)$th rod be replaced by a rigid wall: $u_{J+1} = 0$, then:

$$SEu'_J|_{x=y(J+1/2)} = F_J^r = -K_2 u_J|_{x=y(J+1/2)} - \lambda_2 \dot{u}_J|_{x=y(J+1/2)} - K_1 e^{-\alpha_1 t}\int_0^t e^{\alpha_1 t}\dot{u}_J|_{x=y(J+1/2)}\,dt. \tag{6}$$

The initial conditions are zero, the boundary condition:

$$Eu'_0|_{x=-y/2} = P_0 Q(t), \quad Q(t) = \sin(\omega_* t)H_0(\pi - \omega_* t)H_0(t), \tag{7}$$

where P_0 is the stress magnitude, ω_* is the frequency of action, and H_0 is the step-function of Heaviside.

For the chain of masses, system of equations (3) for $j = 1,..., J-1$ and equations for zero and the *J*th masses were used:

$$m\ddot{x}_0 = K_2(x_1 - x_0) + \lambda_2(\dot{x}_1 - \dot{x}_0) + K_1 e^{-\alpha_1 t}\int_0^t e^{\alpha_1 t}(\dot{x}_1 - \dot{x}_0)dt - SP_0 Q(t);$$
$$m\ddot{x}_J = K_2(x_{J-1} - 2x_J) + \lambda_2(\dot{x}_{J-1} - 2\dot{x}_J) + K_1 e^{-\alpha_1 t}\int_0^t e^{\alpha_1 t}(\dot{x}_{J-1} - 2\dot{x}_J)dt. \tag{8}$$

Study dispersion properties of the chain of masses with springs and viscous elements. Take the Laplace transform (*p* is a parameter) of Eq. (3) at zero initial conditions with respect to time:

$$f^L(p) = \int_0^\infty f(t)e^{-pt}dt, \quad f(t) = \frac{1}{2\pi i}\int_{\alpha-i\infty}^{\alpha+i\infty} f^L(p)e^{pt}dp$$

and the discrete Fourier transform (*q* is a parameter):

$$f^{F_d}(q) = \sum_{j=-\infty}^{j=\infty} f_j e^{iqjy}; \quad f_j = \frac{1}{2\pi}\int_{-\pi/y}^{\pi/y} f^{F_d}(q)e^{-iqjy}dq.$$

The problem is solved in the following way:

$$x^{LF_d} = \frac{P_0 SQ^L}{D(p,q)}, \quad D(p,q) = \frac{mp^3}{K_1} + \frac{mp^2}{\lambda_1} + 4\sin^2\frac{qy}{2}\left(\frac{\lambda_2 p^2}{K_1} + p\left(1 + \frac{K_2}{K_1} + \frac{\lambda_2}{\lambda_1}\right) + \frac{K_2}{\lambda_1}\right), \tag{9}$$

where $D(p,q)$ is the dispersion operator of the system. Substitute $c = c_1 + ic_2$ into the dispersion equation $D(iqc,q) = 0$, where c_1 and c_2 take only real values: c_1 is the phase velocity of waves, and c_2 characterizes attenuation. It follows from an analysis of the dispersion equation that at q, the inequality:

$$c_1 \le y\sqrt{\frac{K_1 + K_2}{m}} = \bar{c} \tag{10}$$

is satisfied, and the phase velocity of infinite-long waves ($q \to 0$) equals:

$$c_1\big|_{q\to 0} = y\sqrt{\frac{K_2}{m}} = \tilde{c}\ . \tag{11}$$

The dependence $c_1(q)$ was determined numerically from the dispersion equations. The calculated results are shown in Fig. 7 ($\lambda_2 = 10^3$ kg/s, $K_1 = K_2 = 5\cdot 10^6$ kg/s^2, $y = 0.1$ m, and $m = 0.3822$ kg). Curves *1 – 5* correspond to $\lambda_1 = 10^5$, 10^4, 10^3, $5\cdot 10^2$, and 10^2·kg/s, respectively.

It is seen from the graph that at some parameters, the wave propagation velocity maximum c_* is reached on medium-long waves ($0 < q_* y < 2\pi$), and it can be higher than the long wave velocity (for example, curves *1*, *2*, and *3*). This difference may be great depending on the problem parameters. By change in λ_1, it is possible to make the propagation velocity of the dispersion-free wave packet vary within $\tilde{c} \le c_* \le \bar{c}$. Note that $\bar{c}$ is approximately 10 times less than the longitudinal velocity in a rod.

NUMERICAL CALCULATIONS AND COMPARISON WITH THE EXPERIMENTS

System of equations (4) was solved with zero initial (5) and boundary (6) conditions using the finite-difference method. Approximation error was minimized by an optimal selection of grid steps with respect to space (h) and time (τ): $c\tau = h$. System of equations (3) and (8) was solved with the same method.

The experimental time-dependences of acceleration of the second and the tenth rods in the system with rigid rubber interlayers are illustrated in Fig. 8*a*, *b* by lines *1*. Lines *2* correspond to the calculated dependences of acceleration on time, that were obtained using an elastoplastic interlayer model with the parameters selected so that the theoretical and experimental data be in satisfactory compliance (Fig. 6, Table 1). Curves *3* were plotted for $K_1 = \lambda_1 = \lambda_2 = 0$, $K_2 = K_{st}$. Under such loading, the calculated results for the rod system and the mass chain coincide. It is evident from a comparison of the theoretical and experimental curves that if only static rigidity of rubber interlayers is taken into account, the theory and experiment show a significant discrepancy.

In this case, the theoretical wave velocity C_{st} is much less than the experimental one C_V . The same is related to the wave attenuation coefficient and the main oscillation frequency.

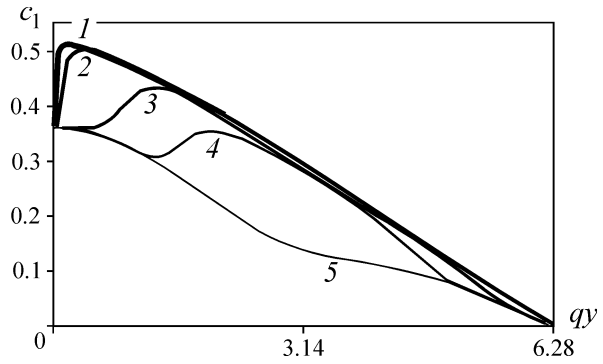

Fig. 7. Phase velocity-to-wave number dependence $c_1(q)$

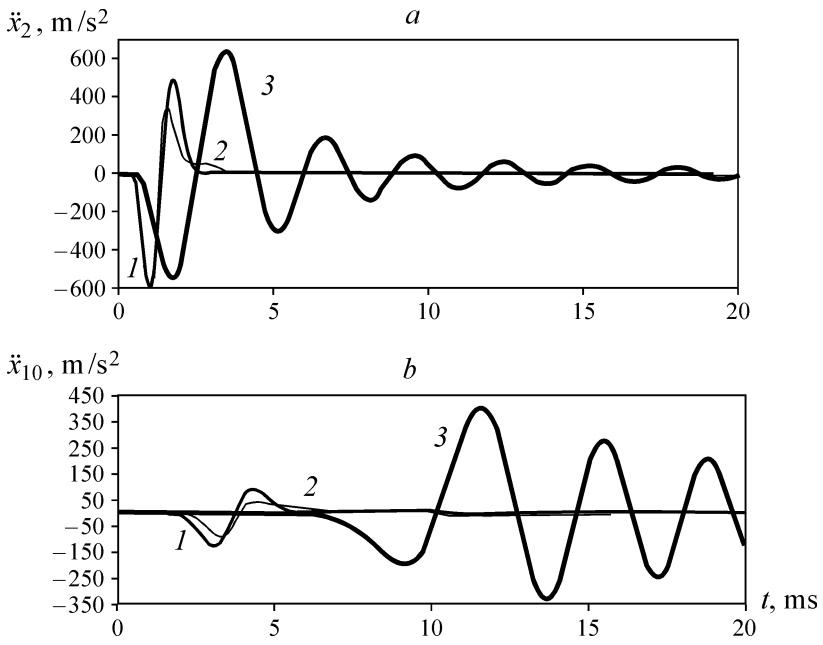

Fig. 8. Time-dependences of acceleration of rods in system with dense rubber interlayers

The values of K_V, λ_1, and λ_2 can be found so that the experimental and theoretical results be close. These parameters are cited in Table 1 together with the propagation velocities of slow waves.

The same calculations were performed using the data of the experiments with interlayers made of porous rubber, linoleum, and foam plastic (Table 1). It is obvious that C_V and C_{st} are rather close only for foam plastic. These values differ to the highest extent in linoleum and dense rubber, where attenuation is also maximal. Note that in these materials, the uniaxial compression curves (similar to those in Fig. 3) have the best pronounced hysteresis under unload. Such hysteresis in porous rubber and foam plastic is far less, and the wave attenuation dependent on λ_2 is weaker.

Finally, the following conclusions can be drawn:

— experimental investigations into the wave propagation in one-dimensional models of block media confirmed the existence of pendulum waves in such media [2];

— velocity, period, and attenuation coefficient of the pendulum waves are heavily dependent on rheological properties of interlayers, such as hysteresis in the extension — compression cycles.

Satisfactory compliance between the theory and experiment has been obtained with the use of viscoelastic model of deformation of interlayers composed of two pairs of elastic and viscous elements that are connected consecutively and in parallel.

The study was conducted with financial support from the Siberian Branch of the Russian Academy of Sciences, Integration Project No. 129, 2003 — 2005.

REFERENCES

1. M. A. Sadovsky, "Natural lumpiness of rock," *Dokl. AN SSSR*, **247**, No. 4 (1979).
2. M. V. Kurlenya, V. N. Oparin, and V. I. Vostrikov, "Generation of elastic wave packets under pulse excitation of block media. Waves of pendulum type U_μ," *Dokl. AN SSSR*, **333**, No. 4 (1993).
3. M. V. Kurlenya, V. N. Oparin, and V. I. Vostrikov, "Pendulum-type waves. Part I: State of the problem and measuring instrument and computer complexes," *Fiz.-Tekh. Probl. Razrab. Polezn. Iskop*., No. 3 (1996).

4. M. V. Kurlenya, V. N. Oparin, and V. I. Vostrikov, “Pendulum-type waves. Part II: Experimental methods and main results of physical modeling,” *Fiz.-Tekh. Probl. Razrab. Polezn. Iskop*., No. 4 (1996).
5. M. V. Kurlenya, V. N. Oparin, and V. I. Vostrikov, “Pendulum waves. Part III: Data of on-site observations,” *Fiz.-Tekh. Probl. Razrab. Polezn. Iskop*., No. 5 (1996).
6. N. I. Aleksandrova, “Elastic wave propagation in block medium under impulse loading,” *Fiz.-Tekh. Probl. Razrab. Polezn. Iskop*., No. 6 (2003).
7. Yu. N. Rabotnov, *Deformable Solid Mechanics* [in Russian], Nauka, Moscow (1988).